Journal of Nuclear Materials 386–388 (2009) 618–621

Contents lists available at ScienceDirect

Journal of Nuclear Materials

journal homepage: www.elsevier.com/locate/jnucmat

Irradiation creep of the US Heat 832665 of V–4Cr–4Ti

Meimei Li [a,*], D.T. Hoelzer [a], M.L. Grossbeck [b], A.F. Rowcliffe [a], S.J. Zinkle [a], R.J. Kurtz [c]

[a] Materials Science and Technology Division, Oak Ridge National Laboratory, Oak Ridge, TN 37831, USA
[b] Nuclear Engineering Department, University of Tennessee, Knoxville, TN 37996, USA
[c] MS P8-15, Pacific Northwest National Laboratory, Richland, WA 99352, USA

A B S T R A C T

The paper presents irradiation creep data for V–4Cr–4Ti irradiated to 3.7 dpa at 425 and 600 °C in the HFIR-17J experiment. Creep deformation was characterized by measuring diametral changes of pressurized creep tubes before and after irradiation. It was found that the creep strain rate of the US Heat 832665 of V–4Cr–4Ti exhibited a linear relationship with stress up to ~180 MPa at 425 °C with a creep coefficient of 2.50×10^{-6} MPa^{-1} dpa^{-1}. A linear relationship between creep rate and applied stress was observed below ~110 MPa at 600 °C with a creep coefficient of 5.41×10^{-6} MPa^{-1} dpa^{-1}; non-linear creep behavior was observed above ~110 MPa, and it may not be fully accounted by invoking thermal creep. The bilinear creep behavior observed in the same alloy irradiated in BR-10 was not observed in this study.

Published by Elsevier B.V.

1. Introduction

Significant progress has been made in developing vanadium alloys for fusion energy applications. The uncertainty in irradiation creep of these alloys is still a major issue due to a limited database. Previous irradiation experiments performed on the reference alloy V–4Cr–4Ti included the ATR-A1 experiment on the US Heat 832665 irradiated up to 5 dpa at 200 and 300 °C in lithium-filled capsules in the Advanced Test Reactor (ATR) [1,2], the HFIR-12J experiment on the same heat irradiated up to 6 dpa at 500 °C in helium-filled capsules in the High Flux Isotope Reactor (HFIR) [3], and a study by Troyanov et al. on a V–4Cr–4Ti alloy irradiated to 3 dpa at 445 °C in the BR-10 fast reactor [4]. Both the ATR-A1 and HFIR-12J experiments used pressurized creep tubes (PCT), while Troyanov used thin-walled tubes loaded in torsion. There is a significant inconsistency in creep strain rate of V–4Cr–4Ti at highest stress levels used in these experiments. The bilinear creep behavior observed in the BR-10 experiment was not found in the ATR-A1 and HFIR-12J irradiation experiments. In the BR-10 experiment the creep rate increased dramatically above 120 MPa, about one-half of the uniaxial tensile yield strength of the irradiated alloy. Additional irradiation creep data are needed to resolve this uncertainty. There is also lack of irradiation creep data at higher temperatures and higher fluences to evaluate the performance limits of this alloy.

This work was undertaken to determine the irradiation creep rates of the US Heat 832665 of V–4Cr–4Ti at 425 and 600 °C. The creep data of PCT specimens at stresses up to 180 MPa are presented, and the results are compared with the earlier irradiation creep data for V–4Cr–4Ti.

2. Experimental

The HFIR-17J experiment was conducted under the Collaborative Testing Program, JUPITER II between the US DOE and the JAPAN MEXT. This experiment contained a total of 28 pressurized creep tube specimens of V–4Cr–4Ti: 14 specimens were fabricated from the US Heat 832665 and the other 14 made from the Japanese NIFS-Heat-2. Seven PCT specimens from each heat were irradiated in each of two lithium-containing subcapsules operated at 425 and 600 °C, respectively. This paper presents the creep data for the US Heat 832665; the irradiation creep data for the NIFS-Heat-2 can be found in the proceedings of this conference [5].

Pressurized creep tube specimens initially had a nominal outer diameter of 4.57 mm, a wall thickness of 0.254 mm and a total length of 25.4 mm. Tube blanks were fabricated from the Batch B drawn tubing of the US Heat 832665, and were exposed to liquid lithium at 800 °C for 168 h and then at 1000 °C for 1 h to reduce oxygen concentration. End caps were made from plate material of the same heat. The end caps were electron-beam-welded to the tube blank, followed by annealing at 1000 °C for 1 h in vacuum before pressurization. Creep tubes were pressurized with high purity helium (99.999%) to develop a desired stress level and sealed by laser welding. The PCT specimens had an average grain size of ~20 μm and contained 161 wppm N, 509 wppm C and 700 wppm O for a total interstitial impurity content of 1370 wppm prior to irradiation. The detailed fabrication process was described in Refs. [6–8].

* Corresponding author. Address: Nuclear Engineering Division, Argonne National Laboratory, 9700 S. Cass Avenue, Argonne, IL 60439-4838, USA. Tel.: +1 630 252 5111; fax: +1 630 252 3604.
E-mail address: mli@anl.gov (M. Li).

0022-3115/$ - see front matter Published by Elsevier B.V.
doi:10.1016/j.jnucmat.2008.12.220

The HFIR-17J experiment was irradiated for 5 reactor cycles for a total of 9930 MWD in a removable beryllium (RB) position of the HFIR. The neutron fast flux level ($E > 0.1$ MeV) was 2–5 $\times 10^{14}$ n/cm^2 s, corresponding to a displacement damage rate of $\sim 4 \times 10^{-7}$ dpa/s. The PCT specimens were held in perforated baskets of a vanadium alloy and sealed within lithium-filled subcapsules. The 425 °C subcapsule was made of 316SS, and the 600 °C subcapsule was made of TZM molybdenum alloy. The primary capsule was surrounded by a Eu_2O_3 shield to absorb thermal neutrons to minimize V to Cr transmutations. The two subcapsules containing PCT specimens were operated at average temperatures of 425 and 600 °C. The temperatures of subcapsules were controlled independently by adjusting the thermal conductivity of the inert gas mixture flowing between the subcapsules and the inner housing. Temperature controls of subcapsules were also dynamically coupled as gas from lower holders was part of the mixture for upper holders. The temperatures were measured by three thermocouples inserted in a thermocouple well that extended from the base of the subcapsule into the specimen assembly and lithium bath. The 425 °C subcapsule was initially designed to operate at a target temperature of 450 °C. A partial blockage of the purge gas line observed in the first cycle of irradiation led to a reduction in the target temperature to ~425 °C. Further degradation of this blockage caused some operational difficulties resulting in this capsule running at slightly lower temperatures, ~418 °C average, for part of the third cycle. The capsule temperature was increased from ~425 to ~445 °C in the last cycle allowing higher argon concentration at the middle 600 °C subcapsule to maintain the temperature at 600 °C. Thus, the temperature of this capsule varied between 418 and 445 °C, and was at an average temperature of 425 °C. The 600 °C capsule operated at 597 ± 3 °C during the duration of the irradiation, though a cooling trend was experienced for this capsule, which required progressively increasing percentages of argon gas to maintain temperature. The design, assembly process and operation of the HFIR-17J experiment are described in detail in Refs. [9–12].

The creep deformation was calculated by the changes of the outer diameters (OD) of PCT specimens before and after neutron irradiation. The specimen OD was measured by a laser profilometer with a resolution of 0.25 μm (~0.005% strain). A tube profile was obtained by measuring the central 12.7 mm of the tube at 500 locations using a helical scan program. The mean OD of a tube was computed by averaging the central 300 measurements to preclude end effects. A standard gauge pin was periodically measured to compensate for any errors from the laser profilometer and the environment. Each specimen was measured three times in a non-consecutive manner, and the average from these three measurements was used to determine the creep strain. The mid-wall effective creep strain of a pressurized creep tube was determined by assuming that the material is incompressible and the deformation caused only by uniform plastic flow. The mid-wall von Mises effective stress of a pressurized creep tube was calculated using the analytical solution of stress state for a thick-walled pressured cylinder [13].

3. Results and discussion

The mid-wall effective strain is plotted as a function of the mid-wall effective stress in Fig. 1 for the PCT specimens irradiated at 425 and 600 °C. Each point represents the average strain of one tube specimen. The zero-stress tubes irradiated at 425 and 600 °C showed effective strains of 0.03% and <0.01%, respectively. Note that the measured strain at zero stress at 425 °C is higher than that at 600 °C, and it comprises a noticeable fraction of the total strain measured at the highest stress level. Precipitation, texture recovery, transmutation or void swelling could introduce positive or negative strain, depending on irradiation conditions.

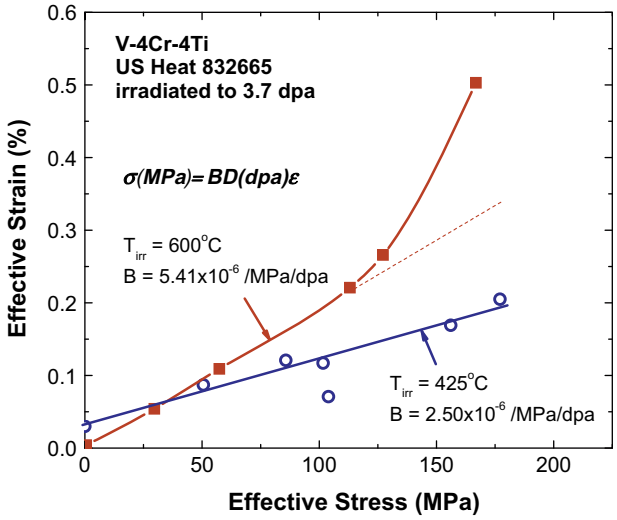

Fig. 1. Irradiation creep data for the US Heat 832665 of V–4Cr–4Ti irradiated to 3.7 dpa at 425 and 600 °C.

The effective strain was proportional to the effective stress up to 177 MPa in the 425 °C irradiated specimens, except the data point at the stress of 104 MPa suggesting tube leakage. Analysis of the data was based on a time-dependent irradiation creep law of the form:

$$\varepsilon = BD\sigma, \tag{1}$$

where ε is the creep strain, σ is the applied stress, D is the damage in dpa (displacement per atom), and B is the creep coefficient. A creep coefficient of 2.50 $\times 10^{-6}$ MPa^{-1} dpa^{-1} was found for irradiation at 425 °C. A linear relation between the effective creep strain and effective stress was observed up to ~110 MPa in the 600 °C irradiated specimens with a creep coefficient of 5.41 $\times 10^{-6}$ MPa^{-1} dpa^{-1}; above ~110 MPa, the effective strain exhibited a non-linear relationship to the effective stress.

Based on an analysis of V–4Cr–4Ti thermal creep behavior, thermal creep can be a significant contributor to the deformation measured following irradiation at 600 °C [14]. It is necessary to separate thermal creep and irradiation creep components to determine if the non-linear stress dependence of creep strain at 600 °C is caused by a thermal creep effect. Due to lack of thermal creep data at the irradiation temperatures, predictions of the thermal creep component using a creep model derived from higher temperature thermal creep tests were attempted. Given the uncertainties of this data extrapolation, these predictions are used as a guide only to estimate the thermal creep effect under the irradiation conditions. Fig. 2 summarizes thermal creep data in both vacuum and lithium environments on V–4Cr–4Ti reported in the literature [13,15,16,2,17–23]. The creep data can be described by a power-law dislocation creep equation:

$$\dot{\varepsilon} = A \cdot \left(\frac{D_{SD}\mu b}{kT}\right) \cdot \left(\frac{\sigma}{\mu}\right)^3, \tag{2}$$

where $\dot{\varepsilon}$ is the creep rate, σ is the applied stress, D_{SD} is the lattice diffusion coefficient (activation energy of 300 kJ/mol), μ the shear modulus, b the Burger's vector, k the Boltzmann's constant, T the absolute temperature, and A is a constant (=0.05 derived from experimental data). Assuming that the same dislocation power-law thermal creep mechanism was operating during neutron irradiation, the thermal creep component at irradiation temperatures of

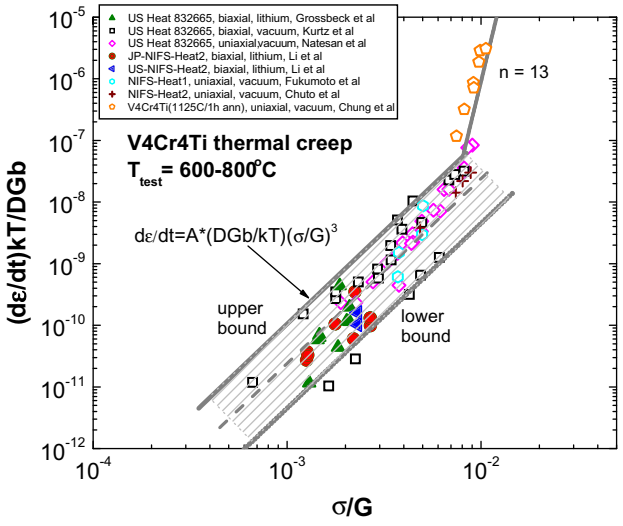

Fig. 2. Summary of thermal creep data for V–4Cr–4Ti tested between 600 and 800 °C in vacuum and lithium.

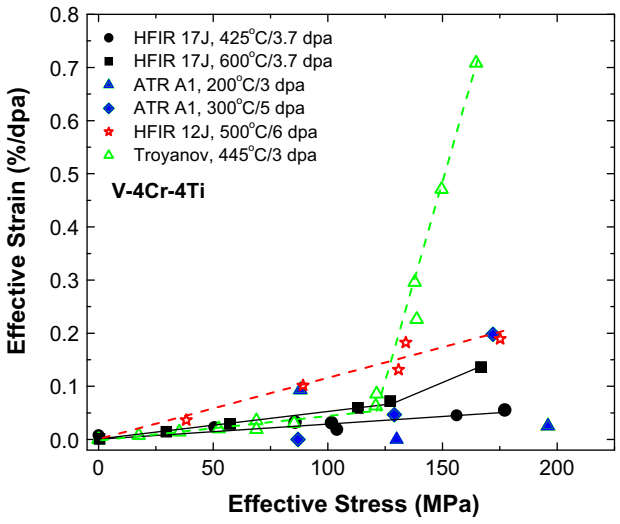

Fig. 4. Comparison of irradiation creep data in the HFIR-17J experiments with the data reported in the literature.

600 °C was calculated using Eq. (2). As thermal creep data vary by nearly one order of magnitude, both a mean value and an upper bound value was used for estimating thermal creep contribution in the overall deformation during irradiation. By subtracting the thermal creep strain from the total train to obtain the irradiation creep strain, total, irradiation and thermal creep strains are plotted as a function of the applied stress in Fig. 3 for V–4Cr–4Ti irradiated at 600 °C. While inconclusive, the analysis using a best estimate and an upper bound estimate suggests that the non-linear stress dependence at 600 °C persisted at high stresses without thermal creep effects. The non-linear stress dependence at high stresses was also observed in HT9 ferritic steel by Grossbeck et al., and was explained using the Preferred Absorption Glide (PAG) mechanism of irradiation creep [24]. The parabolic relation between creep strain rate and stress predicted by the PAG model seems to fit well with the 600 °C-irradiation creep data of the HFIR-17J experiment.

The irradiation creep data in this study are compared with the results of the ATR-A1 and the HFIR-12J experiments on the same heat of V–4Cr–4Ti along with the data reported by Troyanov et al. [4]. The creep strain rate in the unit of %/dpa is plotted against applied stress in Fig. 4. The linearity of irradiation creep rate with stress was observed in V–4Cr–4Ti for stresses < ~120 MPa at irradiation temperatures of 400–600 °C. At lower irradiation temperatures (200–300 °C) in the ATR-A1 experiment, no clear linear stress dependence was observed due to large scatter of creep data. Non-uniform irradiation temperature and displacement damage experienced by the specimens due to space limitation and axial flux gradient may have caused large variations in creep results in ATR-A1 [3]. The significant creep deformation at 172 MPa at 300 °C may indicate higher-order stress dependence. The specimens in the HFIR-12J experiment exhibited a significantly higher creep rate than in the HFIR-17J experiment. The high irradiation creep rate in the HFIR-12J experiment was suggested to arise from the unexpected higher irradiation temperature than the design temperature of 500 °C [25]. The bilinear creep behavior and significantly higher deformation rates at high stress levels reported by Troyanov was not observed in the HFIR-17J experiment, though the irradiation creep rates at lower stress were quite similar in these two experiments.

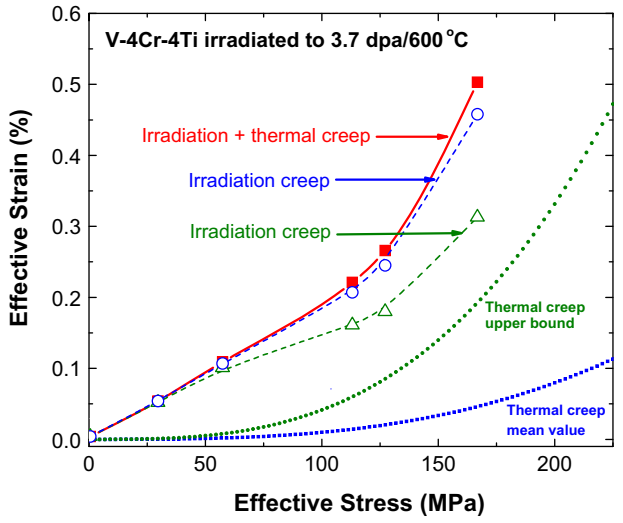

Fig. 3. Irradiation creep strain and thermal creep strain as a function of stress for the US Heat 832665 of V–4Cr–4Ti irradiated to 3.7 dpa at 600 °C. Thermal creep was predicted using a power-law dislocation model. Open circles represent a best estimate, and open triangles represent an upper bound estimate

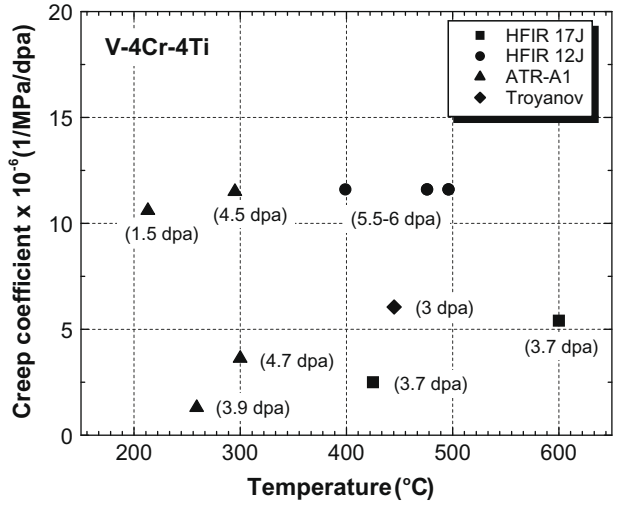

Fig. 5. Creep coefficients as a function of irradiation temperature for V–4Cr–4Ti.

The creep coefficients in the HFIR-17J, HFIR-12J, ATR-A1 experiments and in the Troyanov study are summarized in Fig. 5 as a function of irradiation temperature. The irradiation dose was labeled next to the data points. It is noted that all irradiation creep data were obtained at doses of 3–6 dpa. The measured creep coefficients ranged from 1.4×10^{-6} to 11×10^{-6} MPa^{-1} dpa^{-1}, compared with creep coefficients in bcc ferritic/martensitic steels, $\sim 0.5 \times 10^{-6}$ MPa^{-1} dpa^{-1}, and in fcc austenitic stainless steels, $\sim 1 \times 10^{-6}$ MPa^{-1} dpa^{-1} [26,27]. No clear dependence on irradiation temperature or neutron dose may be drawn from the available data. The variation in creep coefficient of V–4Cr–4Ti is also significantly higher than ferritic/martensitic steels and austenitic stainless steels. Due to complexities of vanadium alloys (such as variations in interstitial contents and texture) arising from fabrication process, heat treatments, effects of environments (e.g. lithium vs. helium) and neutron irradiation on transfer kinetics and distribution of interstitial elements in the solution and precipitates, and irradiation enhanced diffusion and precipitation, no complete explanation of irradiation creep behavior of V–4Cr–4Ti can be furnished without further comprehensive experiments. Irradiation experiments at a range of doses extending to high damage levels are also needed to confirm if there are significant transient effects in vanadium alloys.

4. Conclusions

The major findings of this study are summarized as follows:

1. The creep strain rate of the US Heat 832665 exhibited a linear relationship with the effective stress up to 177 MPa at 425 °C with a creep coefficient of 2.50×10^{-6} MPa^{-1} dpa^{-1}.
2. A linear relationship between creep rate and applied stress was observed below ~110 MPa at 600 °C with a creep coefficient of 5.41×10^{-6} MPa^{-1} dpa^{-1}.
3. A non-linear relationship was observed above ~110 MPa at 600 °C, and it may not be explained by thermal creep only. Further analysis is needed to understand this non-linear creep behavior.
4. The bilinear creep behavior observed in the BR-10 experiment can was not confirmed in the HFIR-17J experiment.

Acknowledgements

The research was sponsored by the Office of Fusion Energy Sciences, the US Department of Energy under contract DE-AC05-00OR22725 with Oak Ridge National Laboratory and under contract DE-AC06-76RLO1830 with Pacific Northwest National Laboratory. The authors would also like to express their great appreciation to L.T. Gibson, M.J. Myers, A.M. Williams, P.S. Tedder, R.G. Sitterson, L.T. Turner, and the personnel in 3525 Material Development and Examination Complex for their technical support.

References

[1] H. Tsai, H. Matsui, M.C. Billone, R.V. Strain, D.L. Smith, J. Nucl. Mater. 258–263 (1998) 1471.
[2] D.S. Gelles, J. Nucl. Mater. 307–311 (2002) 393.
[3] H. Tsai, T.S. Bray, H. Matsui, M.L. Grossbeck, K. Fukumoto, J. Gazda, M.C. Billone, D.L. Smith, J. Nucl. Mater. 283–287 (2000) 362.
[4] V.M. Troyanov, M.G. Bulkanov, A.S. Kruglov, E.A. Krjuchkov, M.P. Nikulin, J.M. Pevchyh, A.E. Rusanov, A.A. Smirnoff, S.N. Votinov, J. Nucl. Mater. 233–237 (1996) 381.
[5] K. Fukumoto, M. Narui, H. Matsui, T. Nagasaka, T. Muroga, M. Li, D.T. Hoelzer, S.J. Zinkle, these Proceedings.
[6] A.F. Rowcliffe, W.R. Johnson, D.T. Hoelzer, Fusion Materials Semiannual Progress Report, DOE/ER-0313/33, 2002, p. 7.
[7] A.F. Rowcliffe, D.T. Hoelzer, W.R.Johnson, C. Young, Fusion Materials Semiannual Progress Report, DOE/ER-0313/34, 2003, p. 6.
[8] A.F. Rowcliffe, D.T. Hoelzer, M.L. Grossbeck, Fusion Materials Semiannual Progress Report, DOE/ER-0313/35, 2003, p. 2.
[9] A.L. Qualls, K.R. Thoms, D.W. Heatherly, R.G. Sitterson, Fusion Materials Semiannual Progress Report, DOE/ER-0313/35, 2003, p. 242.
[10] D.K. Felde, A.L. Qualls, K.R. Thoms, D.W. Heatherly, R.G. Sitterson, R.L. Wallace, Fusion Materials Semiannual Progress Report, DOE/ER-0313/36, 2004, p. 120.
[11] D.K. Felde, R.L. Wallace, Fusion Materials Semiannual Progress Report, DOE/ER-0313/37, 2004, p. 158.
[12] D.K. Felde, R.L. Wallace, Fusion Materials Semiannual Progress Report, DOE/ER-0313/38, 2005, p. 159.
[13] Meimei Li, T. Nagasaka, D.T. Hoelzer, M.L. Grossbeck, S.J. Zinkle, T. Muroga, K. Fukumoto, H. Matsui, M. Narui, J. Nucl. Mater. 367–370 (2007) 788.
[14] Meimei Li, S.J. Zinkle, J. ASTM Int. 2 (2005) 267.
[15] R.J. Kurtz, M.L. Hamilton, J. Nucl. Mater. 283–287 (2000) 628.
[16] R.J. Kurtz, A.M. Ermi, H. Matsui, Fusion Materials Semiannual Progress Report, DOE/ER-0313/31, Oak Ridge National Laboratory, 2001, p. 7.
[17] K. Natesan, W.K. Soppet, A. Purohit, J. Nucl. Mater. 307–311 (2002) 585.
[18] H.M. Chung, B.A. Loomis, D.L. Smith, J. Nucl. Mater. 212–215 (1994) 772.
[19] T. Chuto, N. Yamamoto, J. Nagasaka, Y. Murase, J. Nucl. Mater. 329–333 (2004) 416.
[20] K. Fukumoto, T. Yamamoto, N. Nakao, S. Takahashi, H. Matsui, J. Nucl. Mater. 307–311 (2002) 610.
[21] M.L. Grossbeck, J. Nucl. Mater. 307–311 (2002) 615.
[22] M.L. Grossbeck, Fusion Materials Semiannual Progress Report, DOE/ER-0313/32, Oak Ridge National Laboratory, 2002, p. 6.
[23] K. Fukumoto, H. Matsui, M. Narui, T. Nagasaka, T. Muroga, J. Nucl. Mater. 335 (2004) 103.
[24] M.L. Grossbeck, L.T. Gibson, S. Jitsukawa, L.K. Mansur, L.J. Turner, in: Effects of Radiation on Materials, ASTM STP 1325, 1999, p. 725.
[25] D.L. Smith, Fusion Materials Semiannual Progress Report, DOE/ER-0313/28, 2000, p. 24.
[26] K. Ehrlich, J. Nucl. Mater. 100 (1981) 149.
[27] F.A. Garner, M.B. Toloczko, B.H. Sencer, J. Nucl. Mater. 276 (2000) 123.